CONF-800979--16

LA-UR-80-2840

MASTER

TITLE: METHODS USED IN EVALUATING DATA FOR THE INTERACTION OF NEUTRONS WITH LIGHT ELEMENTS (A < 19)

AUTHOR(S): Leona Stewart

SUBMITTED TO: Nuclear Data Evaluation Methods and Procedures Workshop
Brookhaven National Laboratory
September 22-25, 1980

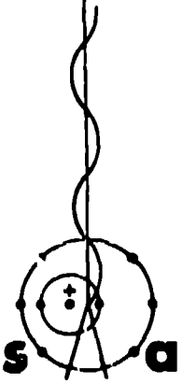

los alamos
scientific laboratory
of the University of California
LOS ALAMOS, NEW MEXICO 87545

Form No. 836
St. No. 2629
1/75

UNITED STATES
ENERGY RESEARCH AND
DEVELOPMENT ADMINISTRATION
CONTRACT W-7405-ENG. 36

METHODS USED IN EVALUATING DATA FOR THE INTERACTION OF NEUTRONS WITH LIGHT ELEMENTS (A < 19)*

Leona Stewart †

Los Alamos Scientific Laboratory, Theoretical Division
University of California
Los Alamos, New Mexico 87545

ABSTRACT

In the interaction of neutrons with light nuclei, many anomalies are observed. In particular, the probability for gamma-ray production is generally small over most of the neutron energy range. On the other hand, ^{6}Li, ^{3}He, ^{10}B, and ^{7}Be have thermal "absorption" cross sections which range from 940 to 48,000 barns. ^{10}B is the only light isotope which has a positive Q for a 3-body reaction, the (n,t2α). As the neutron energy increases, however, 3- and 4-particle direct breakup and sequential formation cross sections dominate the nonelastic for D, T, ^{6}Li, ^{7}Be, ^{10}B, and ^{12}C above a few MeV. For higher-mass isotopes, particle emission (protons and α's) are often the preferred mode for deexcitation of levels excited via (n,n') reactions, where energetically possible. Very few of these partial cross sections have been measured with the necessary precision. Problems are particularly inherent in experiments on negative Q reactions near the 3-body threshold. The many-body problem must be treated as several two-body sequential steps in a theoretical analysis; the emitted particle angular distribution is required as input, but is rarely known. Precise knowledge about individual partial cross sections is often important, especially when neutron multiplication, breeding of fusion fuel, radioactive contamination, depletion or buildup of the target, energy transfer, or time-dependent parameters are required. Specific examples are described for the evaluation of neutron interactions with light elements which employ isotopic spin, inverse reactions, charge-conjugate reactions, and the elastic scattering of charged particles (with Wick's Limit).

---

*Work supported by the U.S. Department of Energy, Division of Reactor Research and Technology, and Offices of Military Application and Basic Energy Science.

† Currently on loan to Oak Ridge National Laboratory, Engineering Physics Department, Oak Ridge, Tennessee 37830.

INTRODUCTION

The evaluation of neutron interactions with light nuclei is of interest for a broad range of applications. Light nuclei are widely used in flux monitors for cross-section standards applications, in the production and use as fusion fuels, as absorbers of low-energy neutrons, as neutron moderators, and as neutron multipliers. Air and water are common neutron shields. Compounds containing hydrogen, carbon, nitrogen, and oxygen are widely employed in research and industry. Of the light stable nuclei, only fluorine plays a minor role in applied programs. Since standards applications are included elsewhere in these proceedings, these cross sections are not covered in this review. Evaluations performed using theoretical models are described in the previous paper, therefore this review includes a tabular summary only of those data (See Table I). This paper will be concerned mainly with briefly describing the many "tools" which can be employed in the evaluation of neutron interactions with light element reactions which greatly enhance the reliability where precise theoretical analyses are not yet available.

METHODS EMPLOYED AS "AIDS"

Various tools can be employed in the evaluation of neutron cross sections. They vary in complexity and detail and several are equally valid for the higher-mass range, though rarely used. These aids are briefly outlined in this section. Examples are chosen to show the results of the use of these tools in the following section. In the context of this review, it would be impossible to give a concise derivation for each theoretical method employed but it is hoped that the simple formulation chosen here will appeal to a wider audience.

Wick's Limit

A minimum value of the zero-degree elastic scattering cross section[7] is called Wick's Limit. It is obtained by assuming that the real part of the scattering amplitude at zero degrees can be neglected. The imaginary part of the scattering amplitude, squared, is simply related by:[7]

$$\sigma(E,0°) > \frac{k^2[\sigma_{TOT}(E)]^2}{(4\pi)^2} > 3.03\times10^{-2}\left(\frac{m_t}{m_n+m_t}\right)^2 [\sigma_{TOT}(E)]^2\, E_{lab}.$$

In evaluating neutron elastic scattering angular distributions to zero degrees, this limit is very useful especially when using charged-particle experimental data and when neutron measurements do not include small angles. It also provides a check on the zero-degree cross sections obtained from Legendre fits to experimental data.

A note of caution should be borne in mind, however, if the zero-degree cross section is automatically set to Wick's Limit. When the real part of the scattering amplitude is identically zero at energy E, the neutron polarization is also identically zero at all scattering angles at that energy.

Charge-Conjugate Reactions

Charge conjugation results from the exchange of the charge of the projectile and target nuclei. Since (n-n), (n-p), and (p-p) forces are the same,* charge-conjugate reactions can be used to great advantage in the evaluation of neutron cross sections and angular distributions for the light nuclei. For ENDF/B-V, the following evaluations widely employed charge-conjugate reactions:

Reaction	Charge-Conjugate	Types of Data
n + D	p + D	Elastic and Non Elastic
n + T	p + ^{3}He	Elastic and Non Elastic
n + ^{3}He	p + T	Elastic and Non Elastic
n + ^{4}He	p + ^{4}He	Elastic †

In the evaluation of the elastic scattering of neutrons by deuterons, n-d data were scarce in number and often of poor quality. Figure 1 shows how the p-d experiments were employed, along with Wick's Limit, in obtaining the shape and magnitude of the n-d angular distribution. A Legendre fit to the n-d data alone left much to be desired. In this case, the minimum in the cross section and the forward-backward peaking were reasonably well represented by p-d scattering, neglecting Coulomb interference at small angles. It was fortuitous that the integral of this curve agreed with $\sigma_{TOT} - \sigma_{NON}$ to within a few mb at 5.6 MeV.

Phase-Space

To complete the evaluation of the n-d interaction, an n-body code was designed to calculate the energy and angle for the D(n,2n) reaction. By assuming equal probability in phase space, the energy distribution in the center-of-mass system of any one of the "n" particles emitted can be represented by:

$$N(E_1)\, dE_1 = \text{Constant} \sqrt{E_1}\, [E_1(\max) - E_1]^{(3n/2)-4}\, dE_1$$

---

*Neglecting Coulomb effects and proton-neutron mass differences.

†For n + ^{4}He, only the elastic channel is open up to 20 MeV.

where $E_i(max)$ is the maximum energy available to particle "i" and depends only on the incident neutron energy and the Q-value of the reaction. The angular distributions, translated into the laboratory reference system, are derived from the above equation. Experimental data for D(n,p)2n and D(p,2p) are essentially all of the (n,2n) spectral information available for the light nuclei. A direct comparison of the experimental D(n,p)2n proton spectra with phase space calculations is shown in Figure 2 for 14.4-MeV neutrons. These calculations are normalized assuming the evaluated $\sigma_{n,2n}$ cross section is 180 mb. In Figure 3, D(p,2p) calculated spectra at 13.9 MeV are compared with the extensive experimental data. The data were smoothed to obtain the solid lines. Note that the experimental data indicate final-state interactions and charge effects between the two identical protons emitted. The general agreement in magnitude is quite good, especially at small angles.

Finally, the sum over neutron energies produces a strong forward peaking of the emitted neutrons as seen in Figure 4. The important conclusion to be drawn is that the assumption of isotropy in the center-of-mass system produces large anistropic distributions in the laboratory system. Near 14 MeV, the 0°/180° ratio is almost 100 for D(n,2n) neutrons.

Inverse Reactions

A reaction and its inverse are directly related through the reciprocity theorem and time reversal invariance. The translation of a reaction to its inverse (or vice versa) involves only the density of states, and the spins and angular momenta of each particle in the entrance and exit channels. Both the cross sections and angular distributions of the reaction products are translated in the same manner.

No experiments were available on the $^3He(n,p)$ reaction below 1 MeV even though the cross section is 5327 barns at thermal energy. Although a 1/v shape and magnitude could be determined from measurements of total cross sections at low energies, it was important to extend the shape to high energies.

Measurements had been made, however, on the inverse reaction:[10,11]

$$p + T \longrightarrow n + {}^3He - 0.764\ MeV,$$

which, when translated into the $n + {}^3He$ system covered the energy range from approximately 5 keV to 2 MeV. These results showed the deviation from 1/v in addition to a plateau near 1 MeV. The measurements are described in Ref. 1.

The classic example of inverse reactions concerns the photodisintegration of the deuteron. Again, cross-section data on this reaction were translated into the $^{1}H(n,\gamma)D$ system in order to extend the evaluation from thermal to 20 MeV. This example was taken from the evaluation of Horsley.[12] The calculations from the inverse reaction compared well with a direct measurement near 14 MeV.

Isospin

The concept of isospin* was first introduced by Heisenberg as a method for labelling two alternative charge states, neutron and proton, by applying the Pauli spin matrix notation. Simply stated, isospin is a shorthand way of representing the charge independence of nuclear forces. A complete derivation cannot be included in this review,† instead, use is made of the formula:

$$T_\zeta = \frac{1}{2}(N - Z),$$

where N is the number of neutrons and Z the number of protons in the nuclei whose mass number is A, usually referred to as "isobaric nuclei". As in physical spin, T_ζ takes on all integer (or half-integer) values between -T and +T.

A diagram[13] for the mass-six isobaric nuclei is shown in Fig. 5. From Eq. (1), the lowest value of isospin (T = 0) is assigned to the ground state of ^{6}Li, which is the stable nucleus. ^{6}He and ^{6}Be form a (T = 1) triplet with the second excited state in ^{6}Li with $J^\pi = 0^+$. Since ^{6}H and ^{6}B do not exist, isospin states with T > 1 have not been observed. Note that isospin states T = 0 and T = 1 are allowed in ^{6}Li while states in ^{6}He and ^{6}Be have only T = 1. States with the same isospin have the same J^π and therefore the same wave function. Since isospin is a good quantum number, it has become a powerful tool in the interpretation of experimental data needed for the evaluation of neutron interactions with nuclei.

COMPARISON OF ENDF/B-V CROSS SECTIONS

The evaluated total cross sections for hydrogen and helium isotopes are shown in Fig. 6. Except for the well-known $P_{3/2}$ resonance in ^{5}He, only broad structure is observed. The broad maximum near 3.4 MeV in ^{4}H has been assigned as a 2^-, T=1

---

*The terms isospin, isotopic spin, and isobaric spin are used interchangeably throughout the literature.

†See the previous paper by G. M. Hale for additional information.

state consistent with its isobaric analogue in ^{4}He and ^{4}Li although a phase-shift analysis implies two and possibly four states to this level (See Ref. 14). Since all of these levels decay by particle emission, unique assignments are difficult. The nonelastic cross sections for D, T, and ^{3}He are smooth.

Total cross sections for ^{6}Li, ^{7}Li, and ^{9}Be are compared in Fig. 7. The peak in ^{9}Be near 2.8 MeV ascribed to two levels is not seen in the evaluation for the (n,2n) cross section (Fig. 8), although the (n,2n)2α reaction threshold is well below this energy, and all levels in ^{9}Be decay by neutron emission. The shape of the evaluated total cross section for ^{9}Be above 10 MeV is not borne out by available experimental data or theory. ^{6}Li is the lowest mass nucleus for which inelastic scattering is possible but all except the 2nd level decay by the emission of α + d. The (n,n'γ) cross sections for the second level were not available except as upper limits but the values assumed are small due to its J^π and T assignment. This T = 1 state corresponds to the isobaric ground states of ^{6}He and ^{6}Be, therefore the shape and magnitude of the ^{6}Li(n,p)^{6}He cross section were assumed. ^{7}Li is the lightest nucleus which shows a significant (n,n'γ) cross section (Fig. 9). This 478-keV level is rarely separable from the elastic peak in a neutron scattering experiment except at low energies so this evaluation was based on γ-ray measurements. Due to the spin and parity of the level, γ-ray emission is isotropic so that an angular distribution measurement was not required. Several problems pertaining to the nonelastic cross sections and the energy-angular distributions of neutron production will be discussed in more detail in the next section.

The total cross sections for ^{10}B, ^{11}B, and C are shown in Fig. 10. Here the structure is significant, especially for C. As noted in Table I, an R-matrix analysis was used for the evaluation of C up to 4.8 MeV. Above this energy, the inelastic scattering from the 4.44-MeV level comes in very strongly and, in fact, shows resonance effects as seen from Fig. 11. The anomaly near 15 MeV is not real. Since ^{10}B is used as a standard and as an absorber at low energies and ^{11}B is not very important, C has been chosen to represent the various partials which make up the total nonelastic cross sections. As seen from Fig. 12, the total (n,n') is made up of the (n,n'γ) and (n,n'3α) reactions. All of the partials show structure below 10-12 MeV. Note the large 4-body cross section which dominates the nonelastic cross section above 14 MeV. In the evaluation, various ^{12}C levels were assigned to allow correlation between the (n,n') neutron energy and angle so that a very small part of the cross section is left in the so-called "continuum" where energy-angle effects are lumped.

The nonelastic cross sections for ^{14}N, ^{16}O, and ^{19}F are shown in Fig. 13. Although (n,n'γ) cross sections become much larger for these nuclei, it should be noted that, at high-excitation

energies, the target often decays via particle emission and these are labeled in ENDF/B-V by flags. Otherwise it would be impossible to check the gamma-ray production cross sections or to calculate hydrogen and helium isotope production induced by neutrons.

CONTINUUM REACTIONS

As mentioned previously, the representation of continuum neutrons for 3- and 4-body reactions is a difficult task for light nuclei. Improvement can be obtained by assuming that a target has bands of excitation energies ($E \pm \Delta E$), with the "real" levels superimposed. These bands can then represent sequential modes of formation and decay of the levels and they preserve the energy-angular distributions of the emitted neutrons. Similar treatment is often made for heavier nuclei when a band of levels could not be effectively separated into each composite part.

The treatment of the ^{6}Li(n,n'd) reaction for 5.74-MeV neutrons is compared with experimental measurements in Fig. 14 at two angles. The experimental data[16] contain the elastic peak while the calculations include several bands of levels plus two real levels at 2.2 and 3.5 MeV. Note that the Version IV evaluation took no account of the energy and angular correlation of the neutrons so that neutrons could be emitted at 134° with energies higher than "allowed" by kinematics for the elastically scattered neutrons. This type of analysis certainly allows energy to be conserved and energy-angular correlations to be used, thereby improving the quality of the evaluation. For more details, s . Ref. 17. The same treatment has been applied in representing the ^{9}Be(n,2n)2α reaction, which is described with many comparisons in Ref. 15. Although the latter results are not ENDF/B-V due to format restrictions,[18] they are available in the ENDF/B format along with uncertainty files, the only requirement is that the (n,n') data be multiplied by two to obtain the total number of neutrons in the exit channel.

NEED FOR IMPROVEMENT OF ENDF/B-V

For the light isotopes, several problems remain of which a few are important and others are interesting. First, and foremost, is the need for a format to represent the error files for the hydrogen and carbon standards. Hydrogen and carbon are scattering standards which infers that the angular distributions of the neutrons must have some statement of error and correlation. The errors on the cross sections, which are all one finds in the files today, are small compared to the uncertainties on the angular distributions.

Second, it is important to note the difference between data measured for an isotope and for a material. For example, is the ^{13}C resonance included in the analysis for ^{12}C? Is the material labeled C or ^{12}C? One knows, a priori, that most of the measurements are made on a material while an R-matrix analysis considers ^{12}C and ^{13}C separately. The reaction cross sections, are usually attributed by virtue of the Q-value to ^{12}C. These comments are not restricted to the carbon evaluation. They are directed, instead, to a clear and concise method for labelling, if one can be found.

Third, a better method is needed for representing (n,2n) and (n,3n) energy and angular spectra for the light nuclei. The data can certainly be calculated today better than they can be represented in the ENDF files. In fact the representation for all continuum reactions for light nuclei needs improvements.

Fourth, to the author's knowledge, several isotopic evaluations are not in reliable condition. The "correct" way to improve the evaluations is not at all obvious from recent measurements. Perhaps the most important are the fuel-breeding reactions, $^{6}Li(n,n'd)$ and $^{7}Li(n,n't)$, above a few MeV.

The $^{6}Li(n,n'd)$ reaction is compared with measurements of the total emission cross section and the Version V evaluation in Fig. 15. While the errors on the measurements are considerable, they certainly do not overlap each other nor, above 6 MeV, the evaluated curve. The Drake data suggest that the evaluation should be higher and the Rosen measurements imply that the evaluation should be lower. Perhaps it should be noted that both Hopkins and Drake measured the total emission spectrum, including the (n,2n) reaction which has a 4.3-MeV threshold, while the α-d star was observed by Rosen.

A consistency check was made by comparing the ^{6}Li elastic scattering measurements with ENDF/B-V (Fig. 16) since all other partials are small compared to the cross sections shown in Fig. 15. This comparison indicates that the elastic could be lowered below about 5.5 MeV, remain the same near 5.5 MeV, and could be lowered appreciably at higher neutron energies, except 14 MeV. The only other obvious alternative would be a large (n,2n) cross section which would be contrary to the imprecise data available and hardly seems likely. It should be noted, however, that energy spectra of the emitted neutrons have been compared among these measurements and the largest discrepancies among the data appear for the emission of neutrons below 1 MeV.

The $^{7}Li(n,n't)$ reaction is shown in Fig. 17. Again, a high and low data set exist except that now the Rosen data are high rather than low. The Swinhoe experiments involved recovering and

measuring the tritium produced in the samples, as did the measurement by Wyman (not represented). The Wyman data reproduced the Rosen data near 14 MeV. Rosen observed the t + α star in emulsions.

When compared to experiment, the ENDF/B-V evaluation on the elastic scattering of neutrons by ^{7}Li (Fig. 16) does not fare so badly since all of the measurements except the first point by Hopkins include the 478-keV inelastic level in the elastic angular distributions. A successful method for correctly representing the angular distributions of the neutrons scattered from this level, is not yet clear.

The nitrogen evaluation could stand some updating for various partial cross sections but these are small contributions to the total nonelastic cross section. The ^{11}B evaluation has not been updated properly since Version I and is perhaps the least reliable of all the evaluations of the light isotopes.

CONCLUSIONS

Although most evaluators of ENDF materials are not particularly concerned with light nuclei, the methods outlined here are often useful in many applications. For example, the X(α,n)Y reaction gives a lower limit on alpha-particle production for the

$$n + Y \longrightarrow \alpha + X$$

inverse reaction for all nuclei since it corresponds to the ground-state transition.

In this review, it has been shown that isospin, charge-conjugate reactions, phase-space arguments, and charged-particle cross sections can often be used to improve the evaluations for light isotope reactions. A precise, theoretical treatment of the complete system, however, is the recommended procedure, where practical.

ACKNOWLEDGMENTS

I wish to express my appreciation for the assistance and cooperation from the Oak Ridge National Laboratory staff in preparation of this manuscript. I would like to thank Patty Boit and Ann Houston for preparing the manuscript.

REFERENCES

1. P. G. YOUNG, "Summary Documentation of LASL Nuclear Data Evaluations for ENDF/B-V," LA-7663-MS, Los Alamos Scientific Laboratory.

2. R. KINSEY, "ENDF-201 ENDF/B Summary Documentation,"BNL-NCS-17541, UC-80, Brookhaven National Laboratory.

3. Brookhaven National Laboratory, "ENDF-300 Standard Reference and Other Important Nuclear Data by the Cross Section Evaluation Working Group," BNL-NCS-51123, UC-34c, ENDF-300.

4. C. Y. FU and F. G. PEREY, "Neutron Scattering Cross Sections of Carbon Below 2 MeV Recommended From R-Matrix Fits to Data," Atomic Data and Nuclear Data Tables 22, 249-267 (1978).

5. D. G. FOSTER, JR. and P. G. YOUNG, "A Preliminary Evaluation of the Neutron and Photon Production Cross Sections of Oxygen," LA-4780 (1972).

6. P. G. YOUNG and E. D. ARTHUR, "GNASH: A Preequilibrium, Statistical Model Code for the Calculation of Cross Sections and Emission Spectra," LA-6947 (1977).

7. E. WANTUCH, "The Scattering of 4.5- and 5.5-MeV Neutrons by Deuterons," Phys. Rev. 84, 169 (1951).

8. J. E. BROLLEY, JR., T. M. PUTNAM, L. ROSEN, AND L. STEWART, "Hydrogen-Helium Isotope Elastic Scattering Processes at Intermediate Energies," Phys. REv. 117, 1307 (1960).

9. A. HORSLEY and L. STEWART, "Evaluated Neutron Cross Sections for Deuterium," LA-3271 (1967).

10. J. H. GIBBONS and R. L. MACKLIN, "Total Neutron Yields from Light Elements Under Proton and Alpha Bombardment," Phys. Rev. 114, 571 (1959).

11. R. L. MACKLIN and J. H. GIBBONS, "On the Absolute Value and Energy Dependence of the ^{3}He(n,p)T Reaction," Proceedings of the International Conference on the Study of Nuclear Structure with Neutrons, Antwerp, 19-23 July 1965, (North-Holland Publishing Co., 1966), p. 498.

12. A. HORSLEY, "Neutron Cross Sections of Hydrogen in the Energy Range 0.001 eV - 20 MeV." Nucl. Data, vol. 2, 243, (1966)

13. F. AJZENBERG-SELOVE, "Energy Levels of Light Nuclei A = 5-10," Nucl. Phy., A320 1-224 (1979).

14. S. FIARMAN and W. E. MEYERHOF, "Energy Levels of Light Nuclei A = 4," Nucl. Phy. A206, 1-64, (1973).

15. P. G. YOUNG and L. STEWART, "Evaluated Data for n + ^{9}Be Reactions," LA-7932-MS (ENDF-283) UC-34c, (1979), Los Alamos National Laboratory.

16. J. C. HOPKINS, D. M. DRAKE, and H. CONDE, "Elastic and Inelastic Scattering of Fast Neutrons from ^{6}Li and ^{7}Li," Nucl. Phys., A107, 139 (1968); and LA-3765, Los Alamos Scientific Laboratory. (Nov. 1967).

17. L. STEWART and P. G. YOUNG, "Evaluated Nuclear Data for CTR Applications," Transactions of ANS Annual Meeting, Toronto, Canada, June 14-18, 1976.

18. R. J. HOWERTON and S. T. PERKINS, "Comments on Beryllium (n,2n) Cross Sections in ENDF/B-IV and -V," Nucl. Sci. Eng. 65, 201 (1978).

TABLE I. EVALUATIONS PERFORMED BY THEORETICAL ANALYSIS

Target/ MAT #	Quantity Predicted	Energy Range	Method Used	Covariance File	Comments	Primary References for Evaluation[a]
1-H-1 1301	$\sigma_{ELAS}(E)$ and $\sigma_{ELAS}(E,\ )$	200 keV to 20 MeV	Yale Phase Shifts	Yes	Actually σ_{tot} was input assuming σ_{tot} [illegible] σ_{ELAS}	LA-766[illegible]-MS (Ref 1) ENDF-201 (Ref 2) ENDF-300 (Ref 3)
2-He-4 127[illegible]	$\sigma_{ELAS}(E)$[b] $\sigma_{ELAS}(E,\ )$ $P(E,\ )$**	10[illegible] to 2[illegible]	R Matrix	No	Analysis performed using [illegible] n + ^{4}He and p + ^{4}He	LA-76[illegible]-MS (Ref 1) ENDF-201 (Ref 2)
3-Li-6 1303	σ_{tot}, σ_{ELAS} $\sigma_{n,t}$, $\sigma_{ELAS}(E,\ )$ $\sigma_{n,t}(E,\ )$, $P(E,\ )$**	10[illegible] to 1 MeV	R Matrix Multi level Multi channel	Yes	[illegible] included [illegible]	LA [illegible] (Ref 1) ENDF [illegible] (Ref 2) ENDF [illegible] (Ref. 3)
5-B-10 1305	σ_{ELAS}, $\sigma_{n,\alpha}$, $\sigma_{n,[illegible]}$ $\sigma(\ )_{All}$ $P(\ )$	10[illegible] eV to 1 MeV	R Matrix Multi level Multi channel	Yes	[illegible]	LA [illegible]-MS (Ref 1) ENDF-201 (Ref 2) ENDF [illegible] (Ref 3)
6-C-12 1306	$\sigma_{ELAS}(E)$ $\sigma_{ELAS}(E,\ )$ $P(E,\ )$**	10[illegible] to 4.8 MeV	R Matrix Multi level Multi channel	Yes	Actually σ_{tot} was input assuming σ_{tot} [illegible] σ_{ELAS}	Unpublished (Ref 4) ENDF-201 (Ref 2)
7-N-1[illegible] 1307	$\sigma_{ELAS}(E)$ $\sigma_{ELAS}(E,\ )$ $P(\ )$**	10[illegible] eV to 5.4 MeV 6-[illegible] MeV	R Matrix [illegible]	No	Only [illegible] data available were σ_{tot} and $P(\ )$.	LA [illegible] (Ref 1) ENDF [illegible] (Ref 2) LA [illegible] (Ref. 6)
8-O-16 1276	$\sigma_{ELAS}(E)$ $\sigma_{ELAS}(E,\ )$ $\sigma_{n,\alpha}(E)$ $\sigma_{n,\alpha}(E,\ )$	10[illegible] eV to 5.7 MeV	R Matrix Multi-level Multi channel	Yes	^{13}C([illegible]) data included in analysis. Also σ_{tot} assumed equal to σ_{ELAS}	LA [illegible] (Ref 5) LA [illegible] (Ref 1)

[a] See these primary references which refer to previous references and often full documentation. A complete list of the appropriate references would number in the hundreds and is therefore omitted here.
[b] For n + ^{4}He, σ_{ELAS} [illegible] σ_{tot} over this energy range.
** Although $P(E,\ )$ data were used as input and calculated values output, the ENDF/B format has no provision for th[illegible] information.

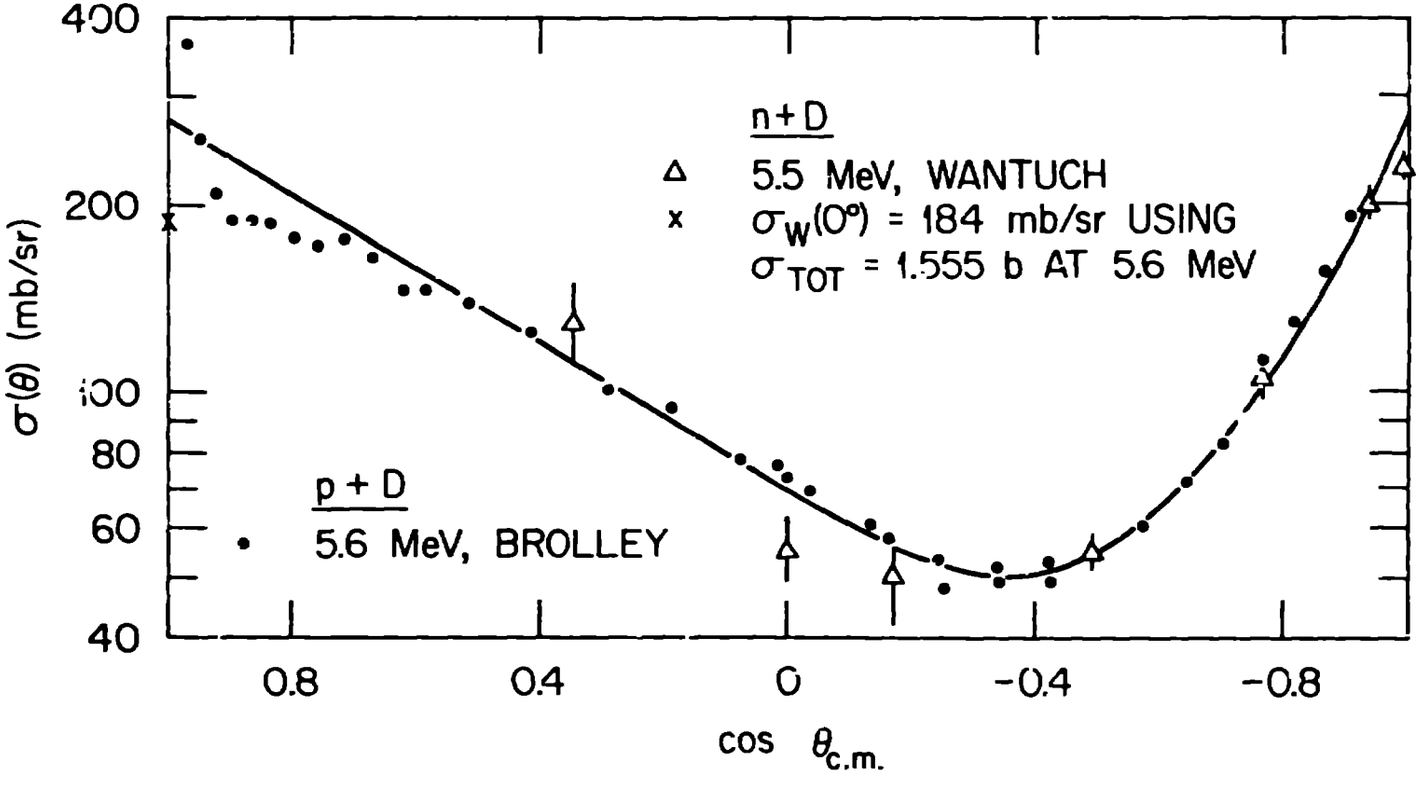

Fig. 1. Elastic scattering of deuterons by neutrons and protons near 5.5 MeV. The experimental data are given in Ref. 7 and Ref. 8.

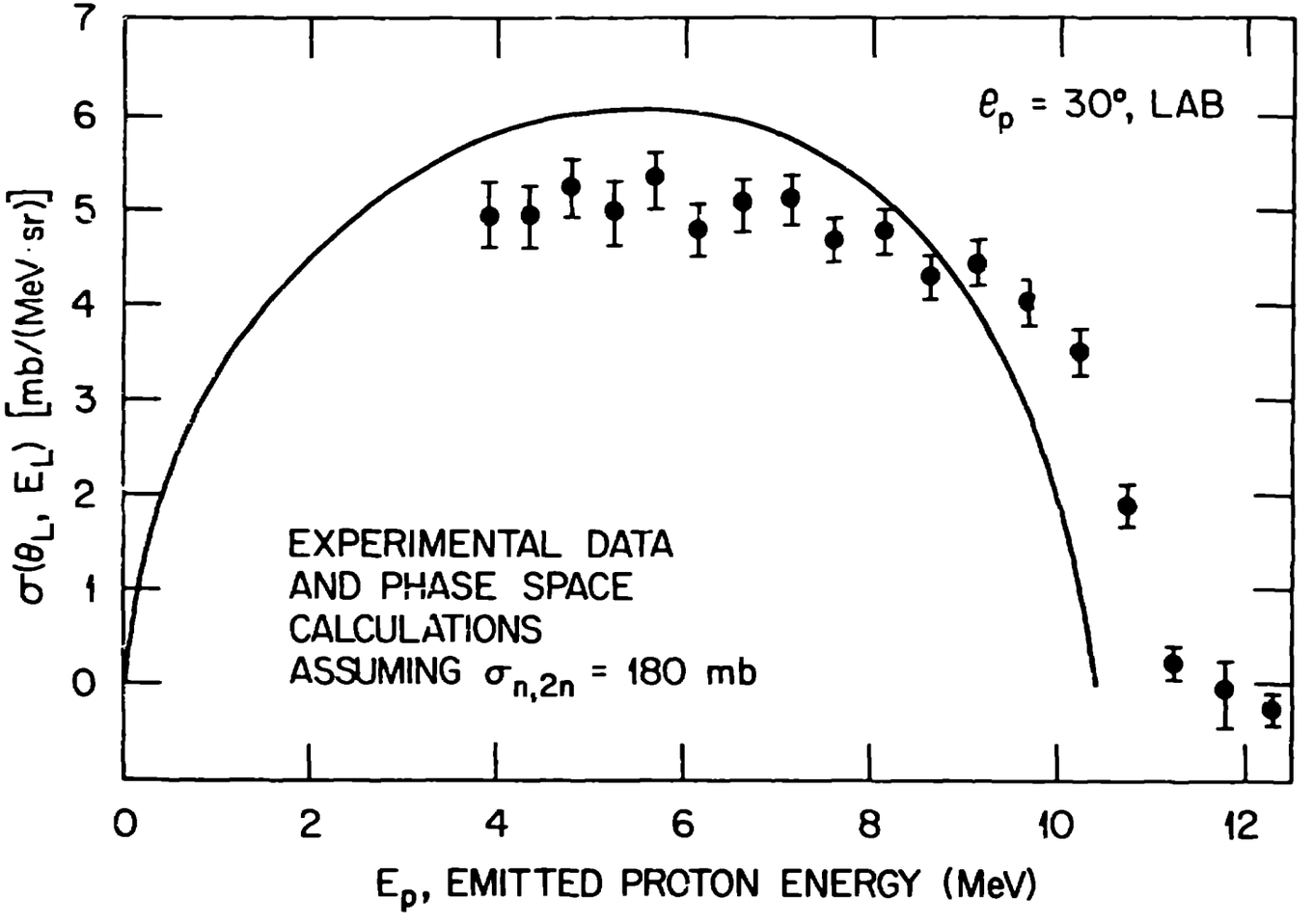

Fig. 2. Proton spectra from the D(n,p)2n reaction at 14.4 MeV compared to 3-body phase space calculations (See Ref. 9 for complete details).

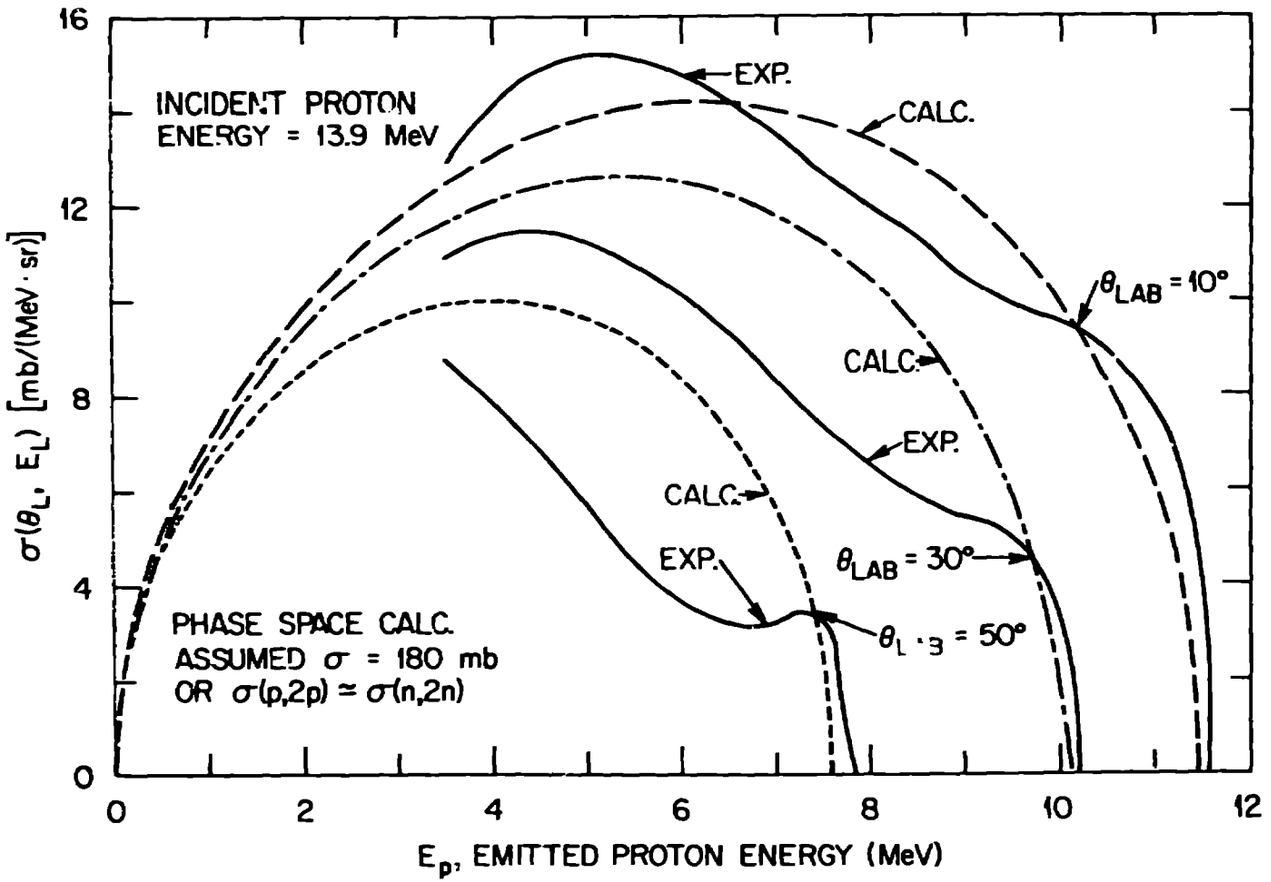

Fig. 3. Proton spectra from the D(p,2p)n Charge-Conjugate Reaction for 13.9-MeV protons compared to Phase Space Calculations (See Ref. 9 for complete details).

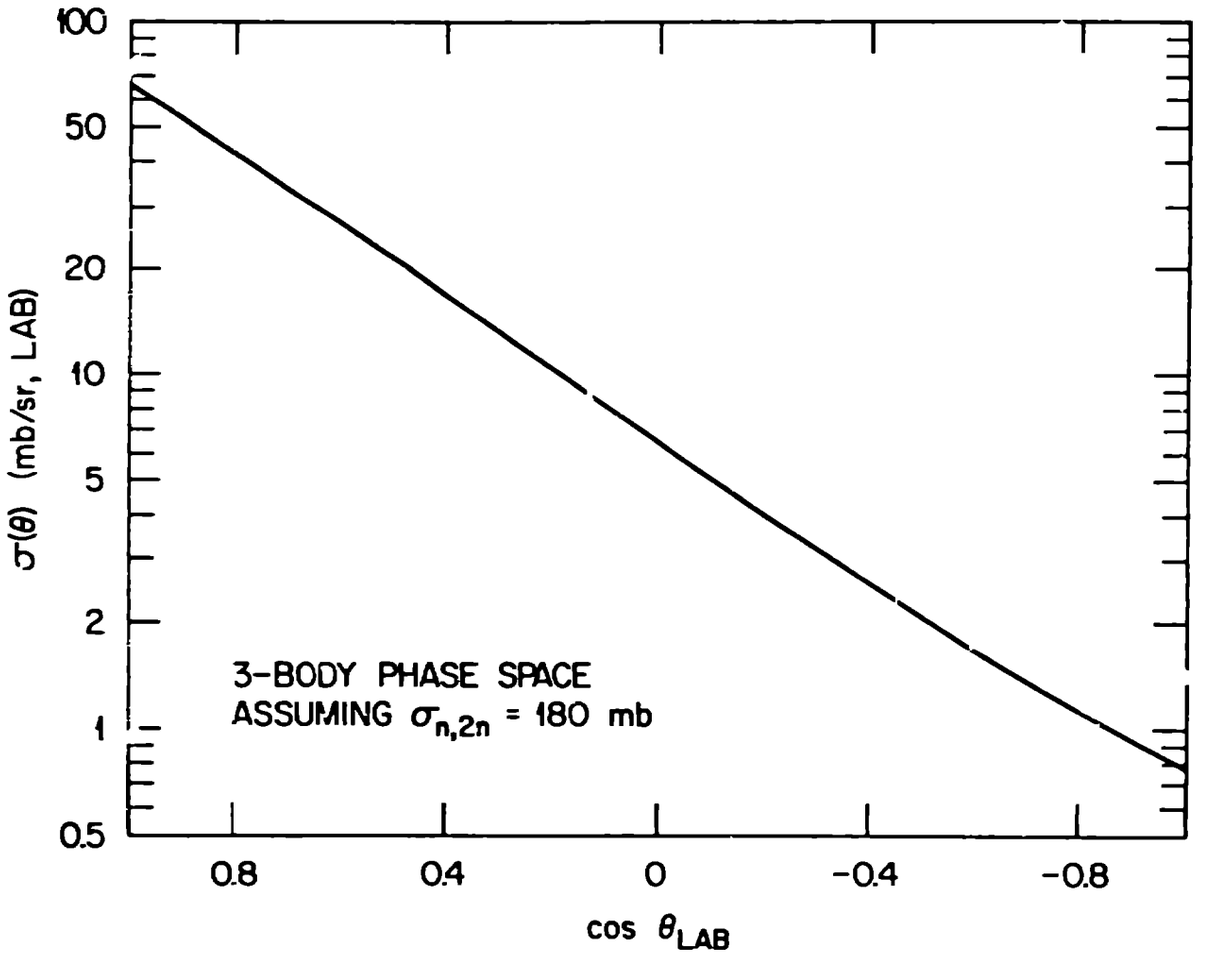

Fig. 4. Angular distribution of the D(n,2n) neutrons near 14 MeV in the laboratory reference system, assuming isotropy in the center-of-mass system.

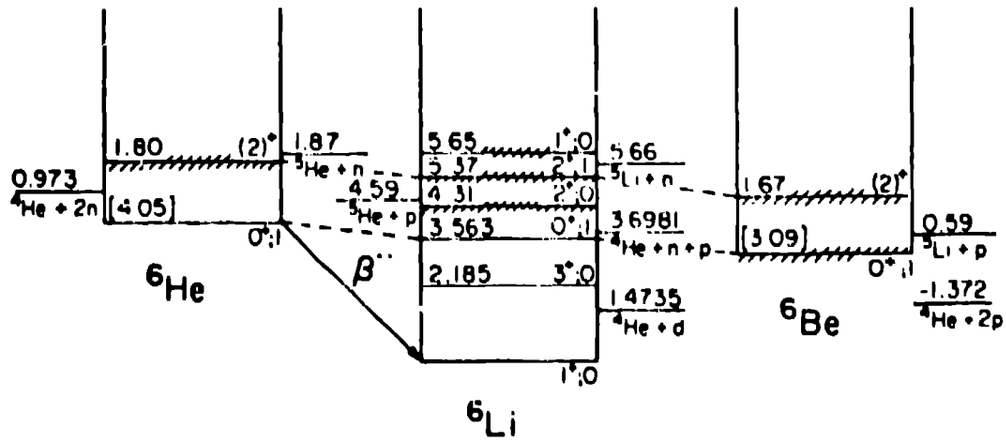

Fig. 5. Comparison of the Isospin Configuration for A = 6 (these data were taken from Ajzenberg-Selove, Ref. 13).

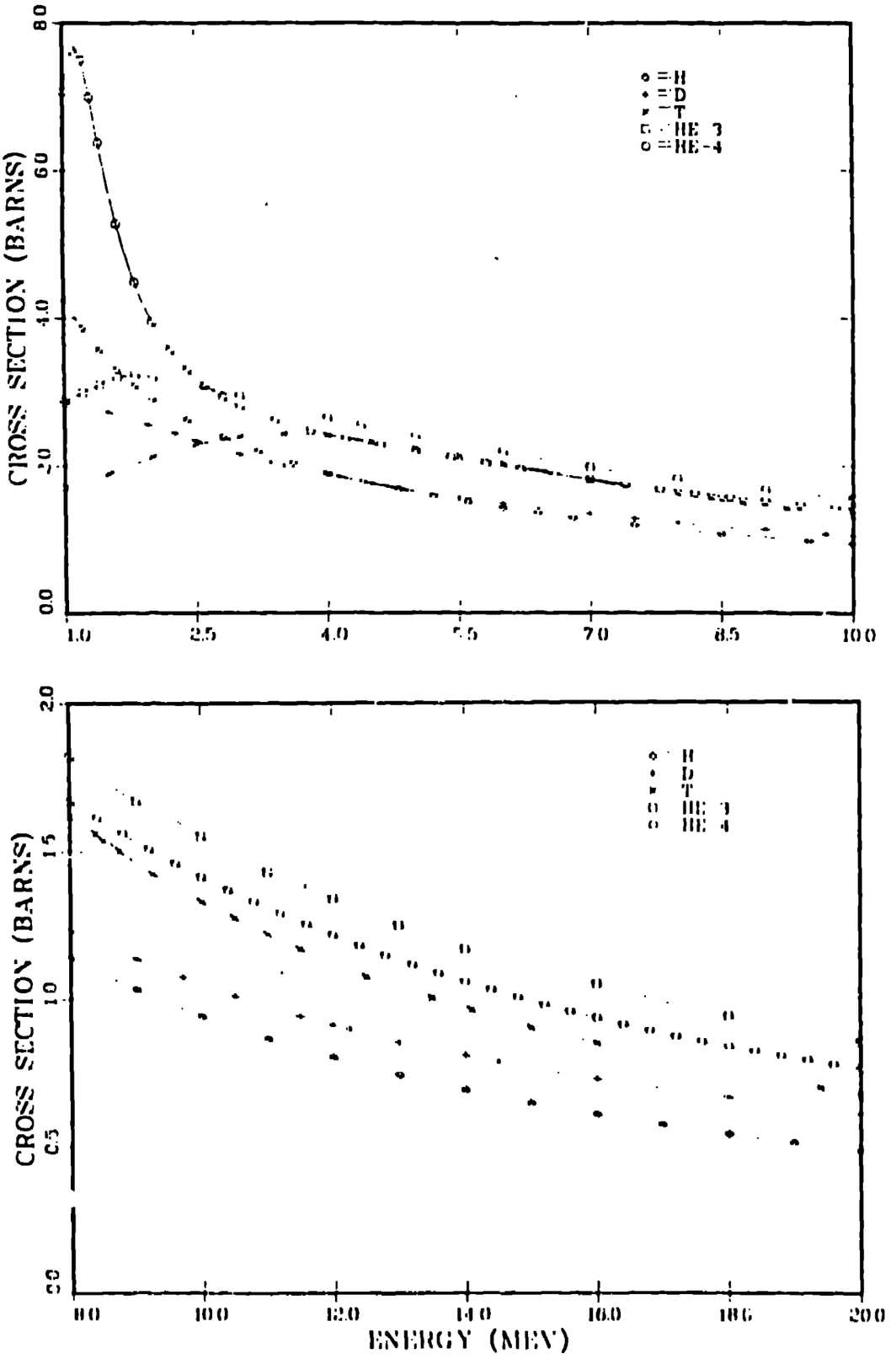

Fig. 6. Evaluated total cross sections for ENDL/B-V for the hydrogen and helium isotopes.

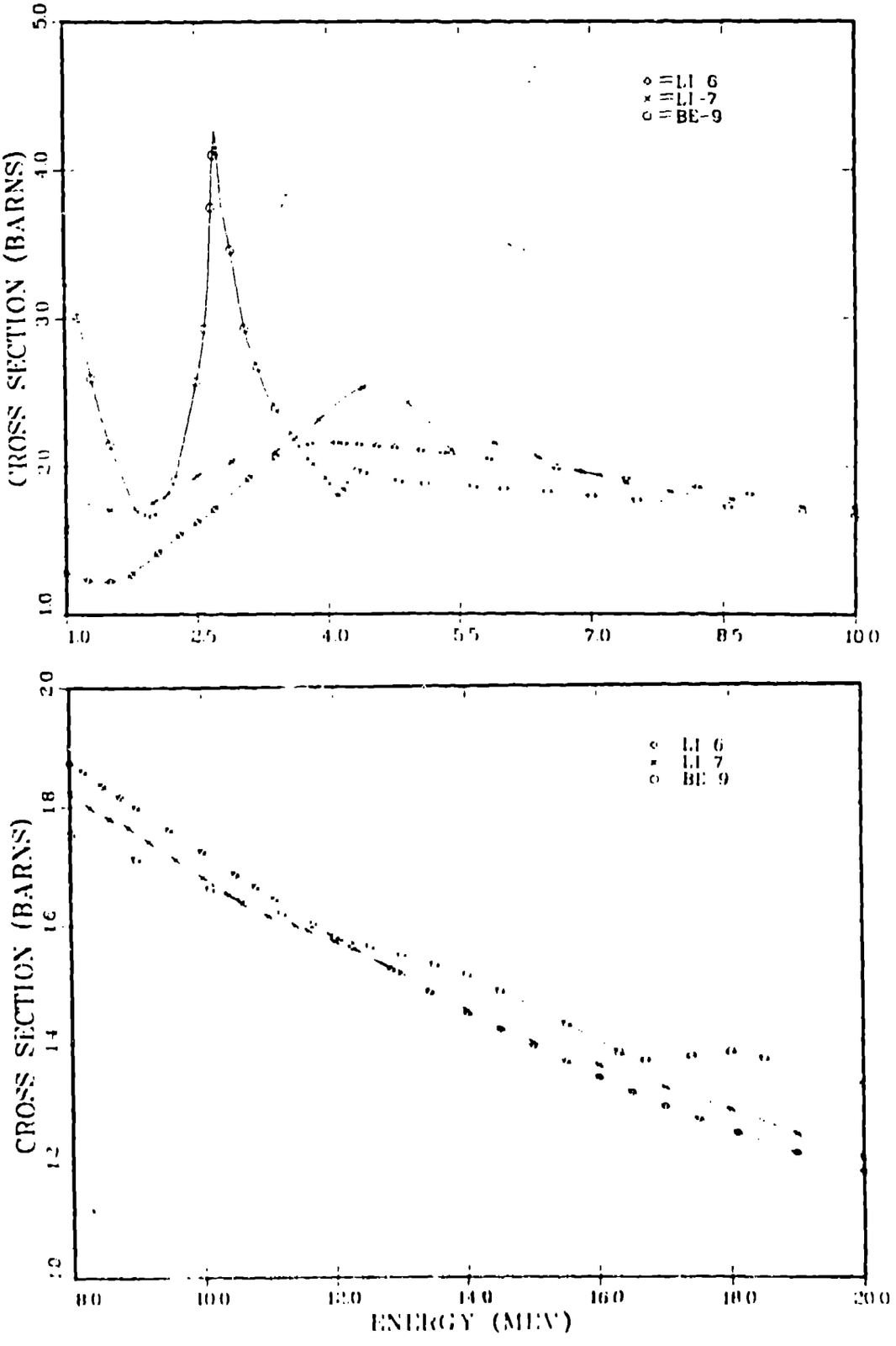

Fig. 7. Evaluated total cross sections for ENDF/B-V for ^{6}Li, ^{7}Li, and ^{9}Be. The structure in ^{9}Be above 12 MeV [illegible]

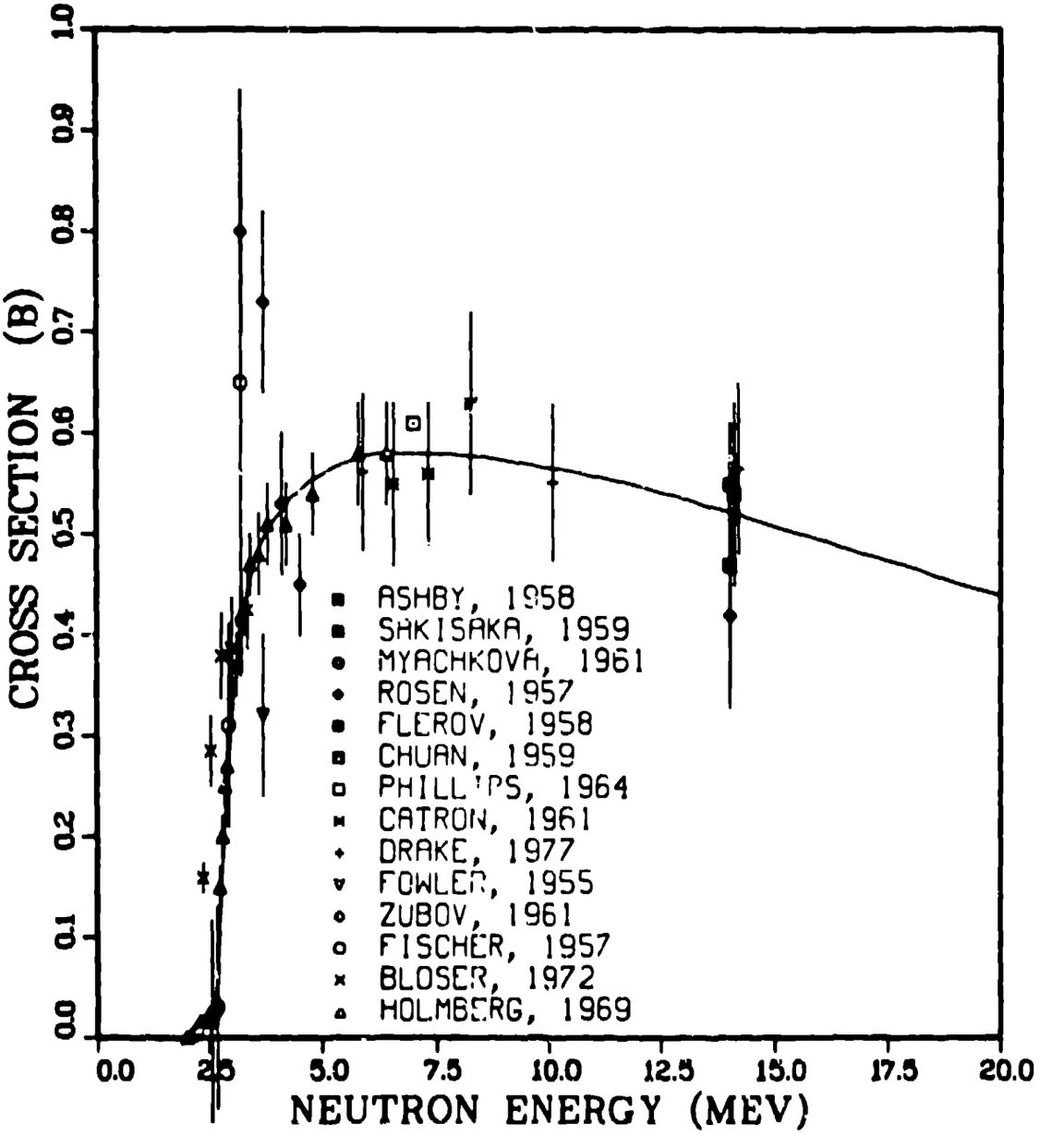

Fig. 8. Measured and evaluated $^{9}Be(n,^{3}n)$ cross sections from threshold to 20 MeV. The solid curve is ENDF/B-V. The experimental data presented here are described in Ref. 15.

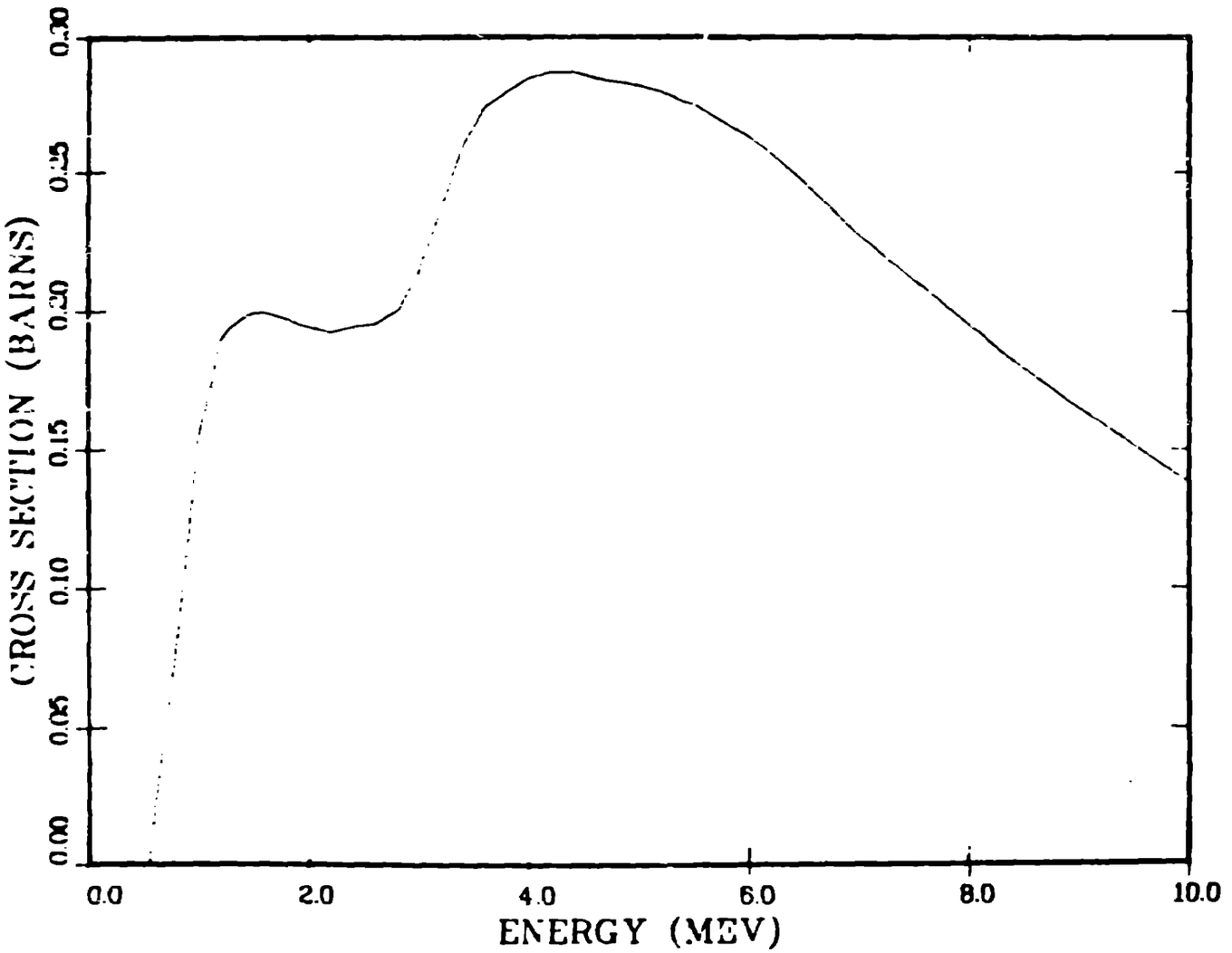

Fig. 9. The $^{7}Li(n,n')$ cross section corresponding to the first excited state in ^{7}Li at 478 keV. All other levels in ^{7}Li decay via particle emission. This cross section steadily decreases to approximately 70 mb at 20 MeV.

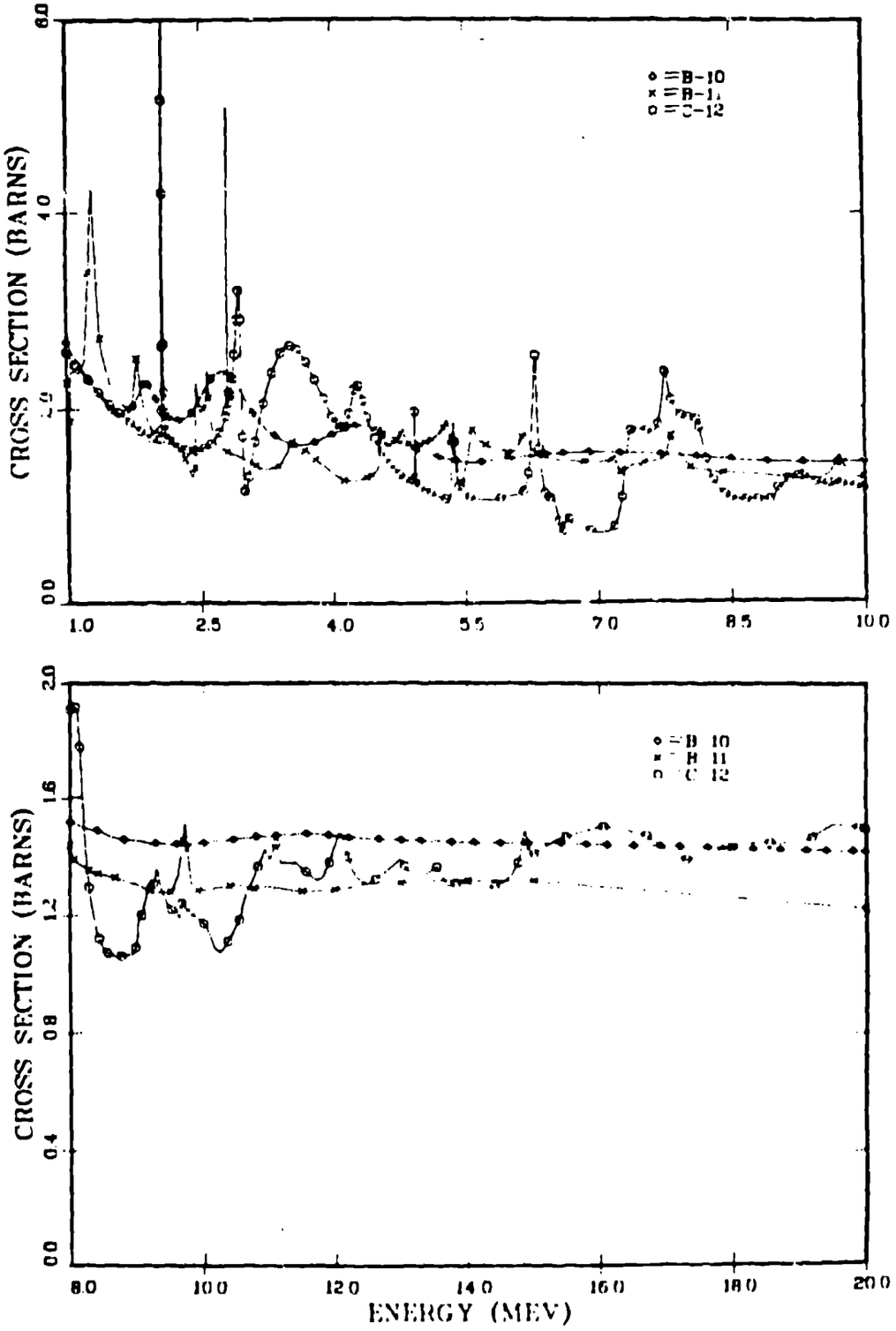

Fig. 10. Evaluated total cross section for ENDF/B-V for ^{10}B, ^{11}B, and ^{12}C.

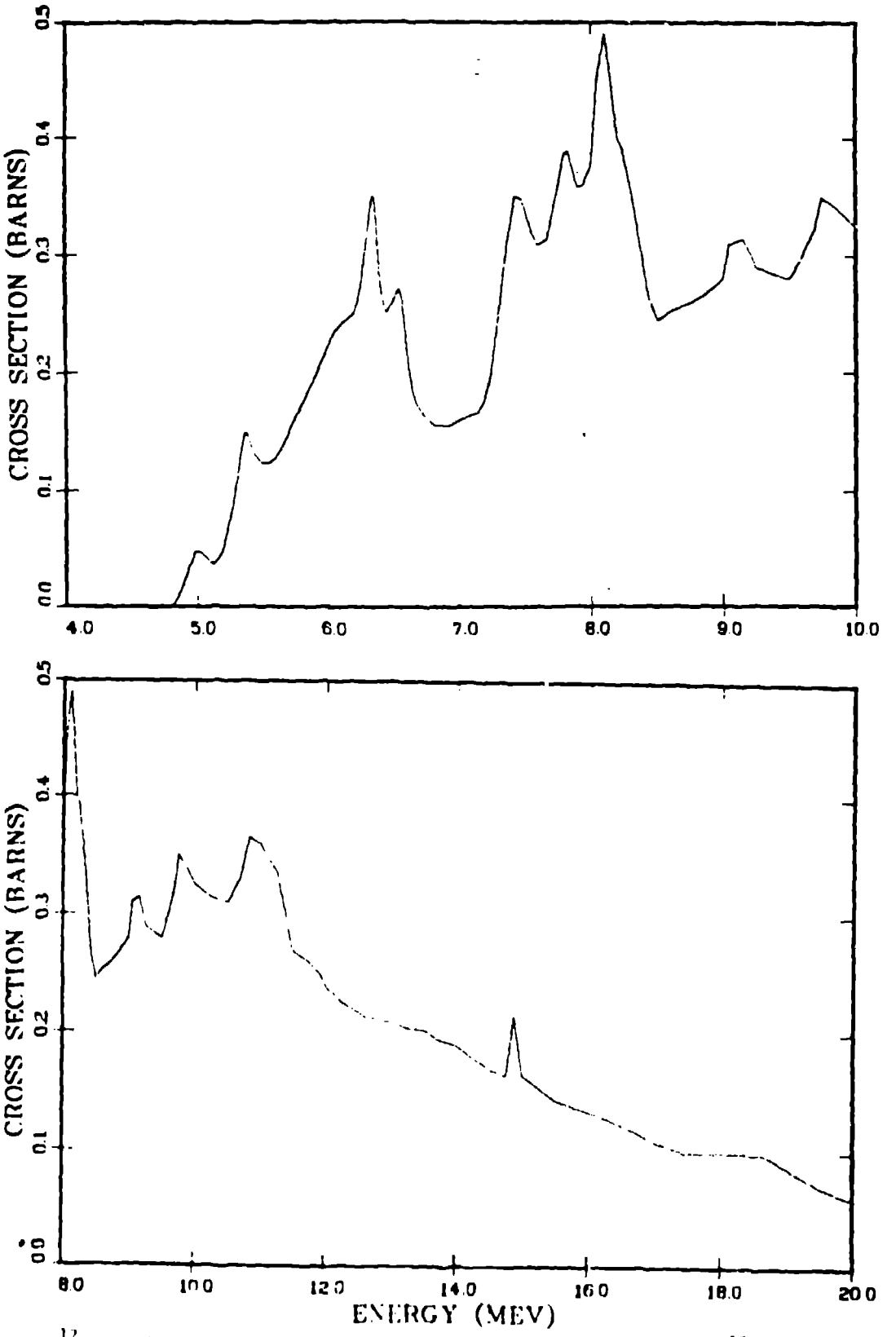

Fig. 11. The $^{12}C(n,n'_1)$ cross section corresponding to the first excited state in ^{12}C at 4.4 MeV. All other states in ^{12}C decay via particle emission.

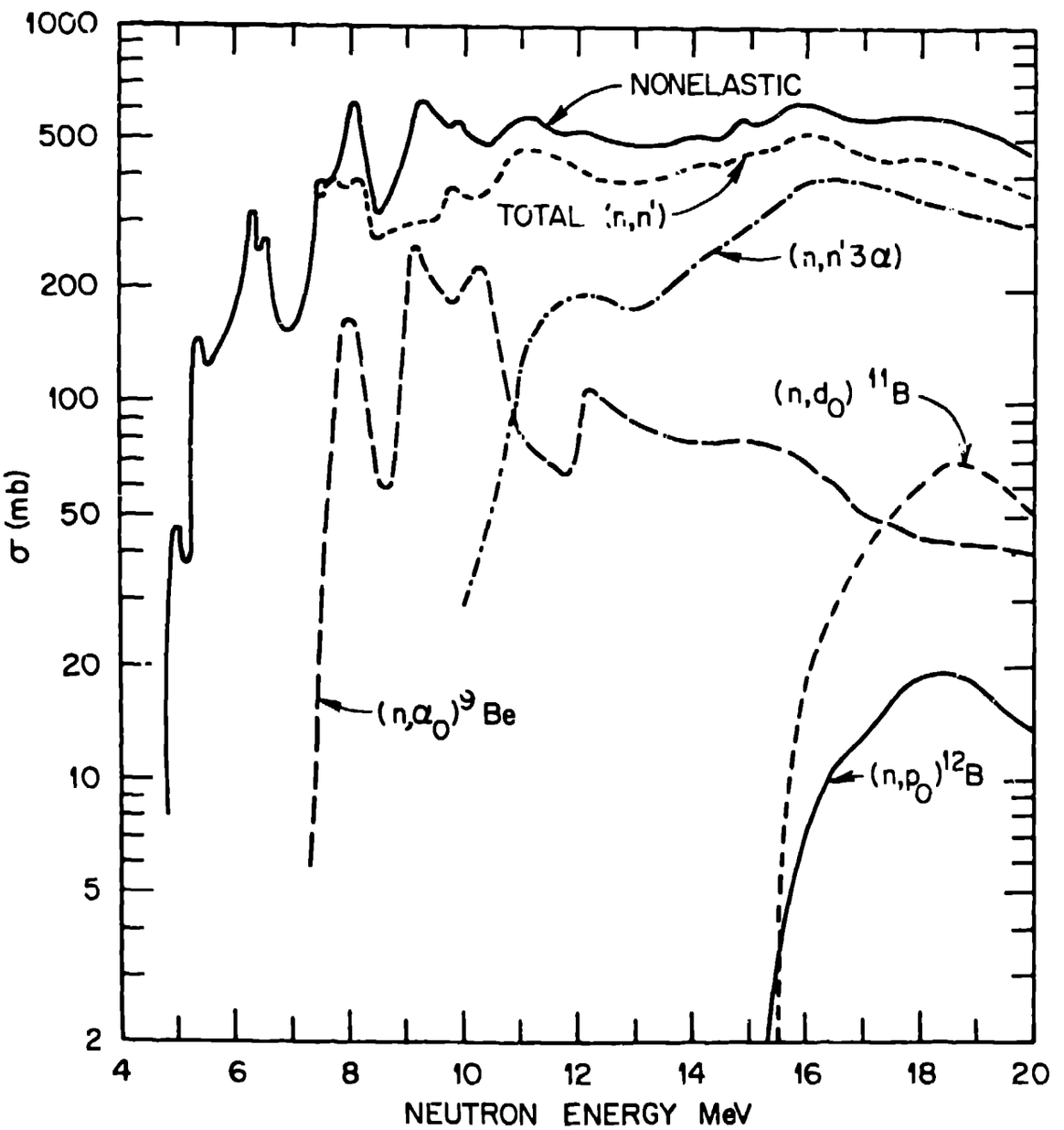

Fig. 12. The evaluated nonelastic cross sections for ^{12}C showing structure in the individual partials at low energies and the large cross section for 4-body breakup at higher neutron energies.

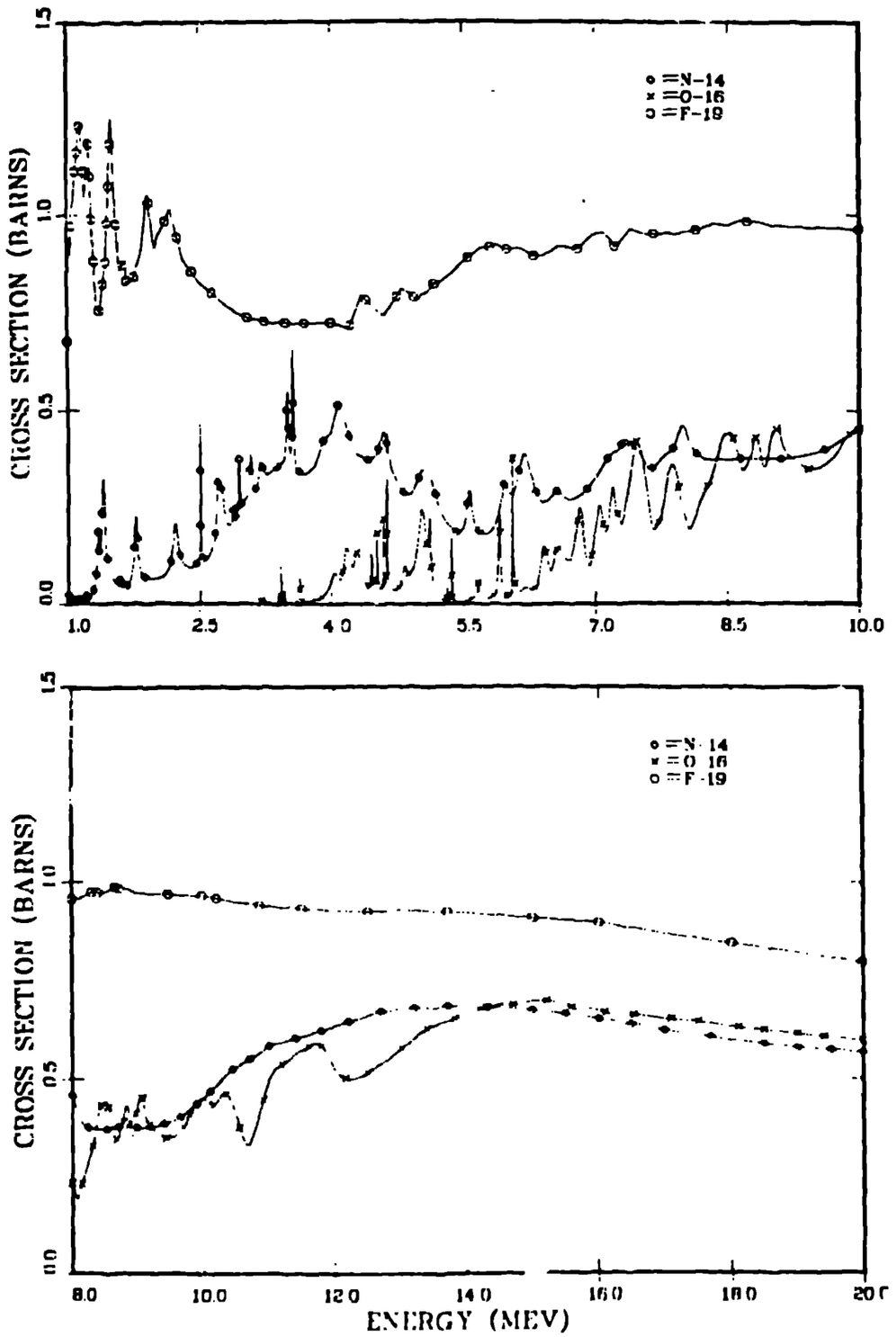

Fig 13. Structure observed in the nonelastic cross sections for ^{14}N, ^{16}O, and ^{19}F.

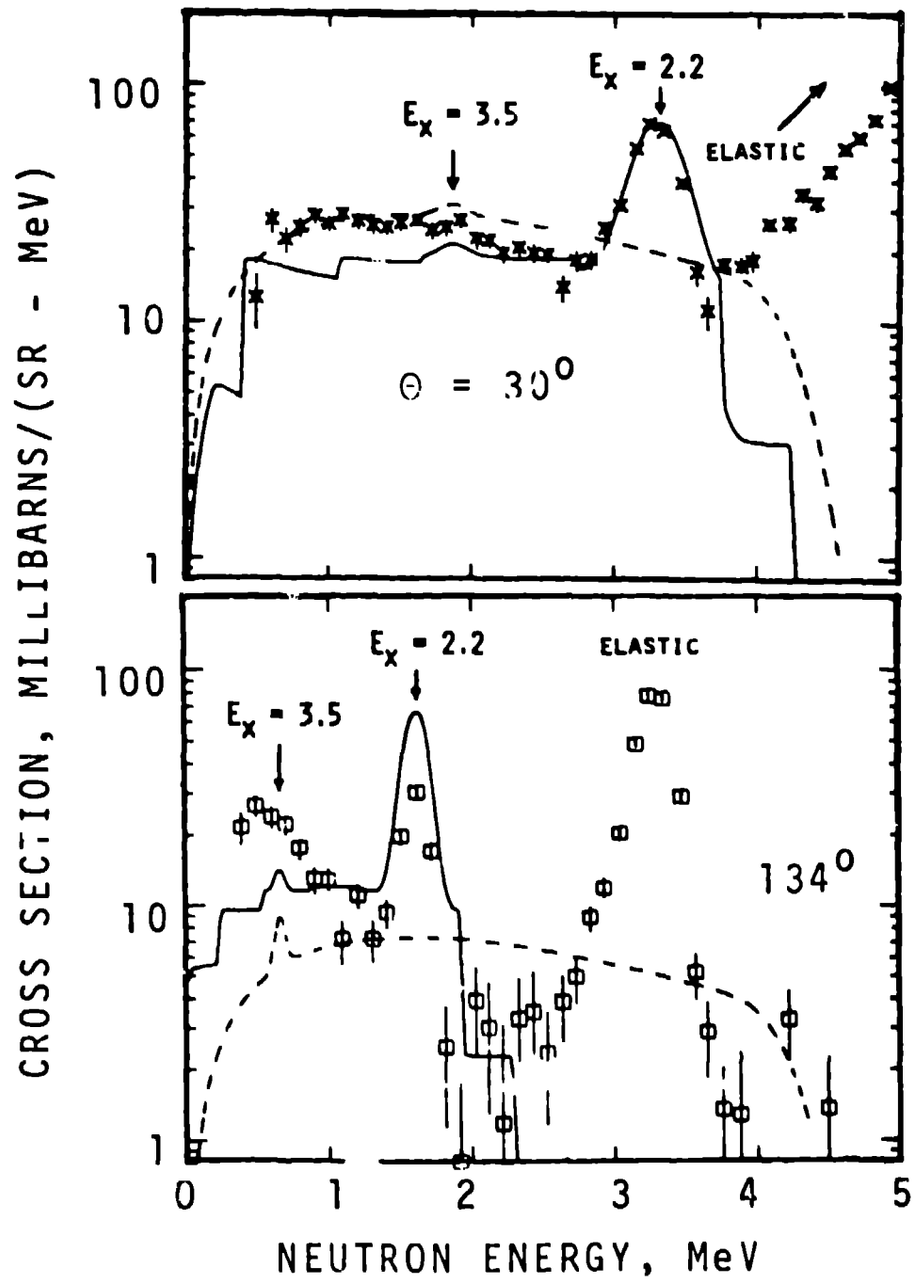

Fig. 14. Experimentally observed neutron spectra from 5.74-MeV neutrons scattered by ^{6}Li. The solid curve (ENDF/B-V) obtained by assuming bands of excitation energies in addition to the "real" levels at 2.2 and 3.5 MeV. The experimental data[16] include the elastic peak while the curves represent only the (n,n'). The dashed curve was taken from ENDF/B-IV.

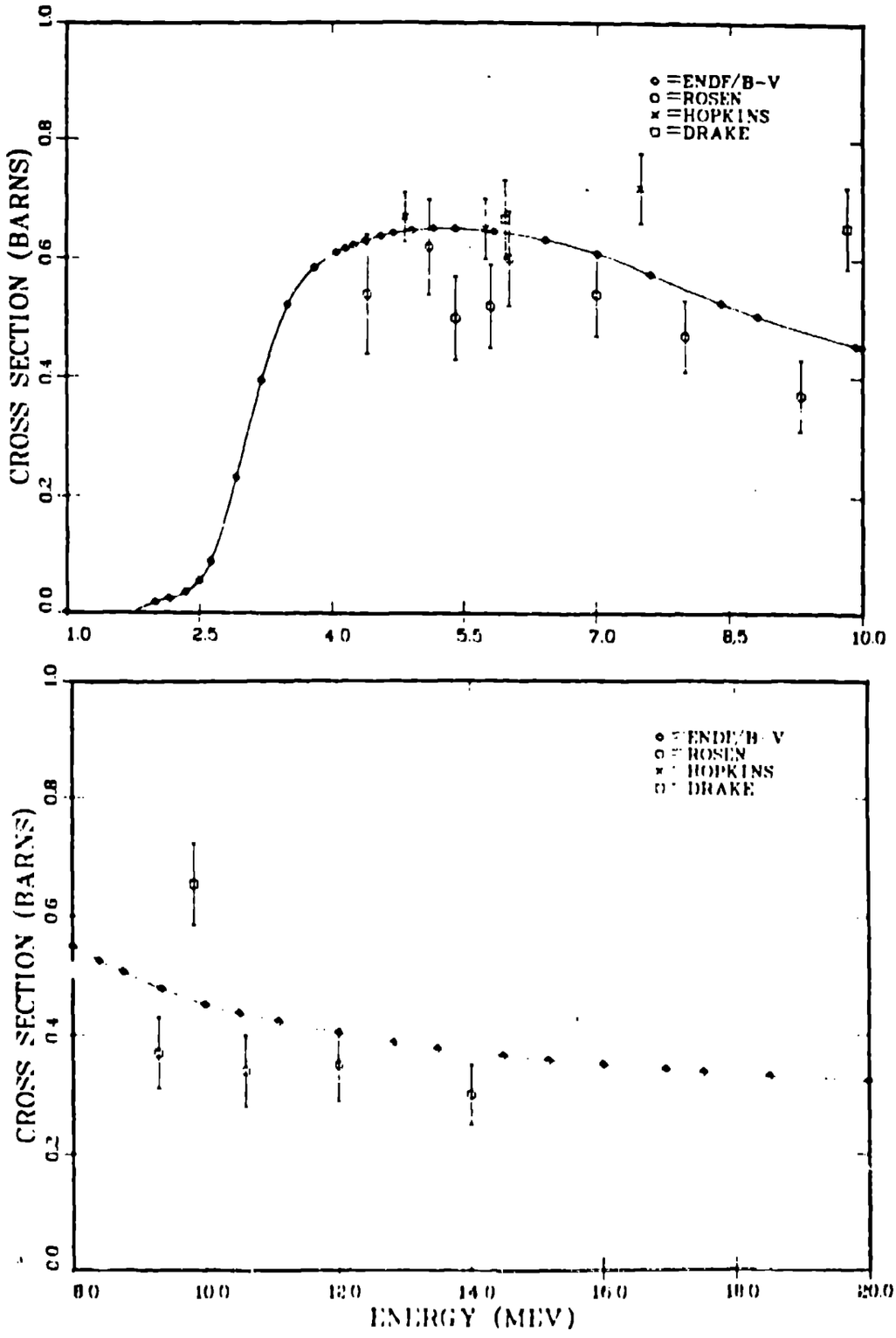

Fig. 15. Comparison of ENDF/B-V with experimental measurements on the $^{51}V(n,n')$ cross sections.

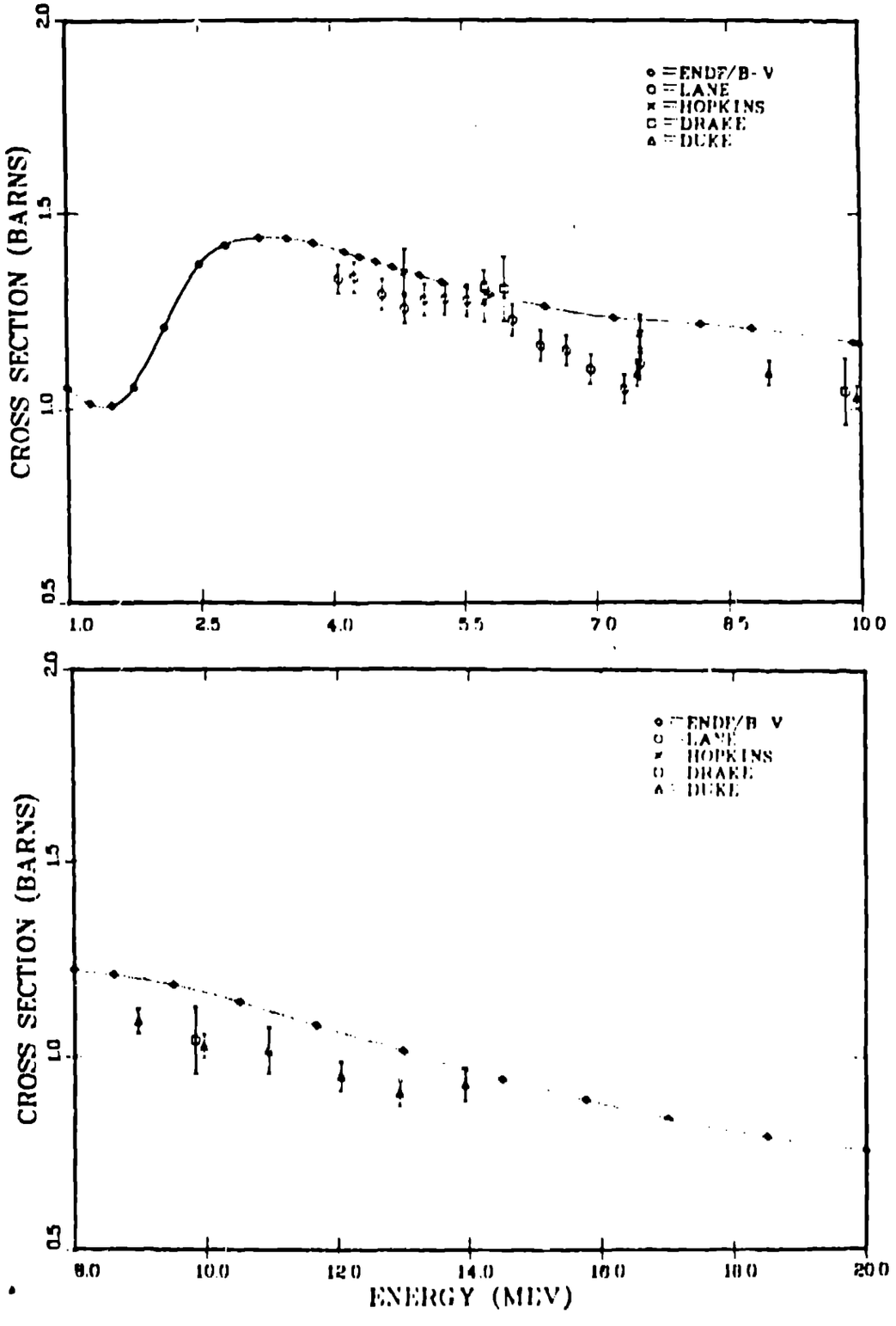

Fig. 16. Comparison of the ENDF/B-V evaluation with the experimental data of neutron elastic scattering on ^{11}B.

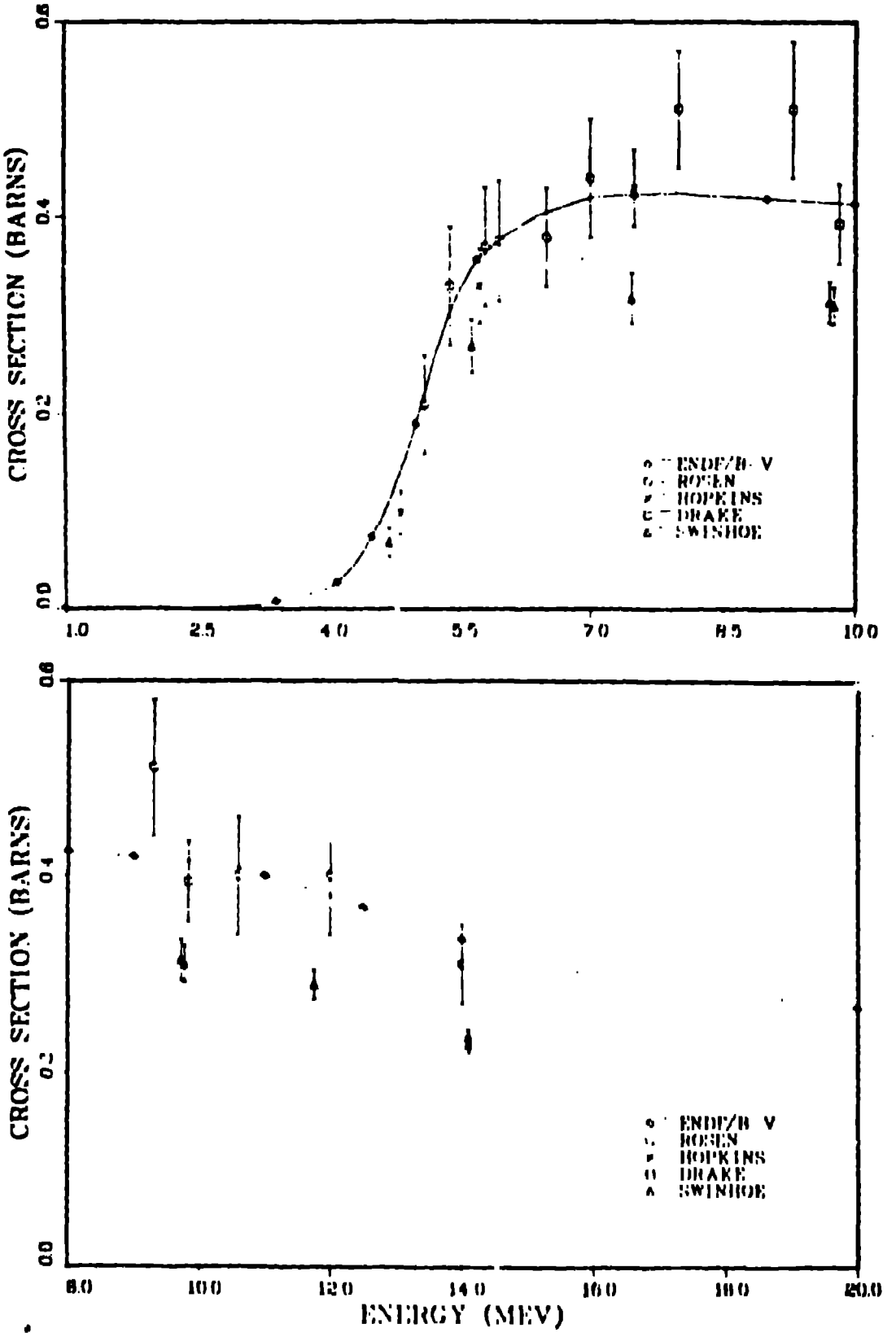

Fig. 17. Comparison of the experimental data on $^{7}Li(n,n'\gamma)$ reaction with ENDF/B V.

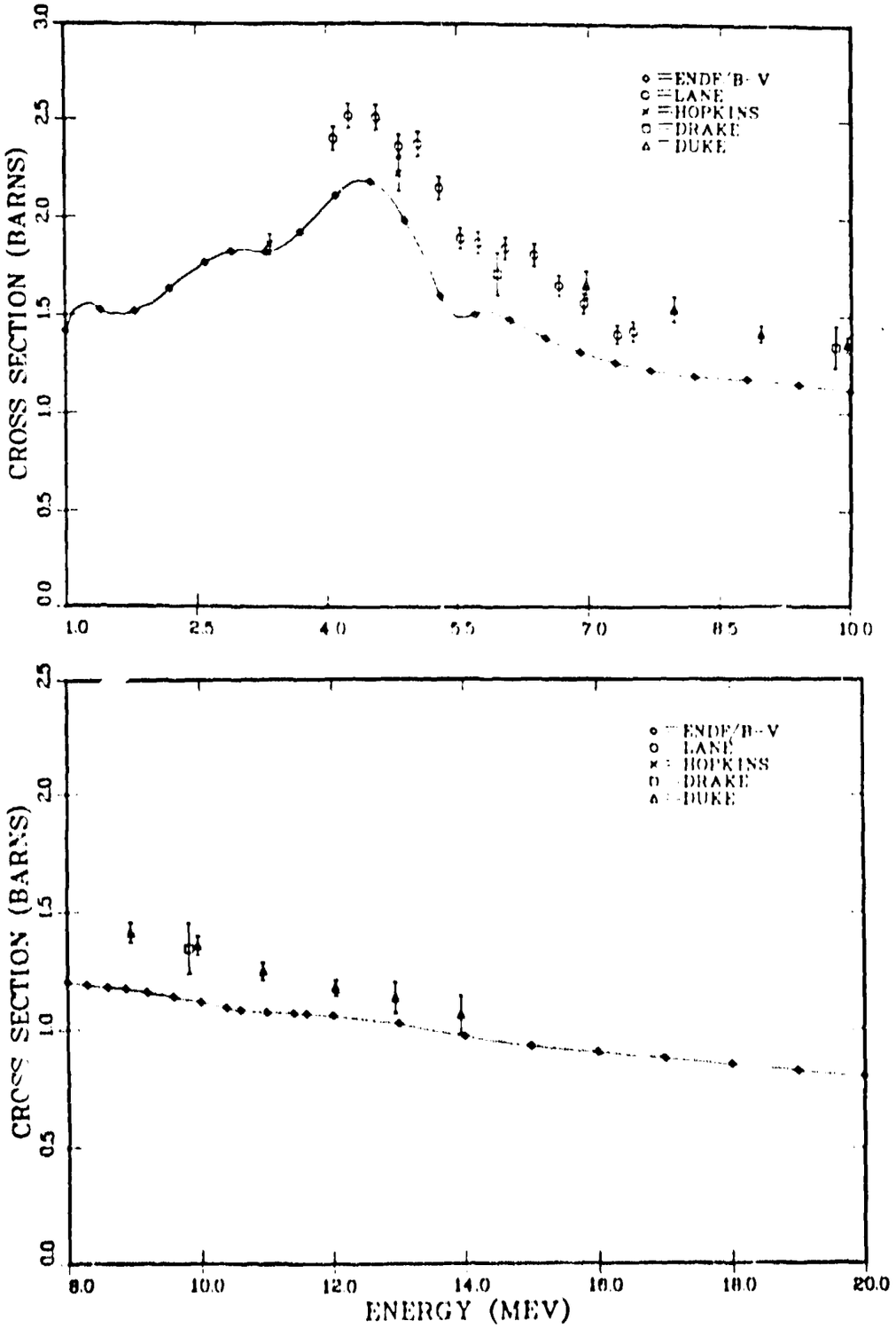

Fig. 18. Comparison of measurements of the elastic scattering of neutrons by ^{7}Li with ENDF/B-V. Here the experiments include the $(n,n'\gamma)$ reaction shown in Fig. 9, except for the point of Hopkins[16] at the lowest energy.